A Phase Field Modeling Approach of Crack Growth in Materials with Anisotropic Fracture Toughness

Christoph Schreiber[1]
Applied Mechanics, Technische Universität Kaiserslautern, Germany

Tim Ettrich
Technische Universität Kaiserslautern, Germany

Charlotte Kuhn
Faculty 7, Universität Stuttgart, Germany

Ralf Müller
Applied Mechanics, Technische Universität Kaiserslautern, Germany

Abstract

Within this contribution, we present a diffuse interface approach for the simulation of crack nucleation and growth in materials, which incorporates an orientation dependency of the fracture toughness. After outlining the basic motivation for the model from an engineering standpoint, the phase field paradigm for fracture is introduced. Further, a specific phase field model for brittle fracture is reviewed, where we focus on the meaning of the auxiliary parameter differentiating between material phases and the coupling of such a parameter to continuum equations in order to obtain the characteristic self organizing model properties. This specific model, as will be explained, provides the phenomenological and methodical basis for the presented enhancement. The formulation of an appropriate evolution equation in terms of a Ginzburg-Landau type equation will be highlighted and several comments on sharp interface models will be made to present a brief comparison. Following up on the basics we then introduce the formulation of a modified version of the model, which additionally to the handling of cracks in linear elastic materials under quasi static loading is also capable of taking into account the effect of resistance variation with respect to the potential crack extension direction. The strong and also the weak forms of the respective governing equations corresponding to the developed anisotropic phase field model are presented. Utilizing the weak formulation as starting point for the discretization of the two fields (displacement field and the phase field), the computational framework in terms of finite elements is introduced. We finally explain several test cases investigated within simulations and discuss the corresponding numerical results. Besides examples, which are set up to illustrate the general model properties, a comparison with crack paths obtained by experimental investigations will be presented in order to show the potential of the developed phase field model.

2012 ACM Subject Classification Applied computing → Physical sciences and engineering

Keywords and phrases Phase field modeling, Brittle fracture, Anisotropic fracture toughness, Finite elements

Digital Object Identifier 10.4230/OASIcs.iPMVM.2020.9

Funding Funded by the Deutsche Forschungsgemeinschaft (DFG, German Research Foundation) - 252408385 - IRTG 2057.

[1] corresponding author

2nd International Conference of the DFG International Research Training Group 2057 – Physical Modeling for Virtual Manufacturing (iPMVM 2020).
Editors: Christoph Garth, Jan C. Aurich, Barbara Linke, Ralf Müller, Bahram Ravani, Gunther Weber, and Benjamin Kirsch; Article No. 9; pp. 9:1–9:17
OpenAccess Series in Informatics
OASICS Schloss Dagstuhl – Leibniz-Zentrum für Informatik, Dagstuhl Publishing, Germany

1 Introduction

One of the important branches of engineering is the field of fracture mechanics. Dealing with failure of technical components and structures several aspects must be considered. Crucial in that regard is crack initiation, determination of critical loads for the onset of crack growth or also the prediction of crack paths or patterns. In order to ensure a design, that combines safety, reliability and also economical aspects, fracture mechanic principles as they are proposed in e.g. [8] or in many other textbooks are incorporated. However, these principles and derivations are often based on simplified assumptions. For complex structures fracture mechanic principles are evaluated applying computational methods as for instance finite elements. Generally, the two alternative approaches are sharp interface approaches on the one hand and diffuse interface approaches on the other hand. Sharp interface approaches either have to adopt a growing crack surface via incremental remeshing algorithms (see e.g. [10]) or are based on so-called enrichment functions, which then often cause conditioning problems, in order to model propagating cracks (see e.g. [24]). The latter is referred to as extended or generalized finite element method. In contrast, within diffuse interface approaches cracks are represented by a smeared approximation. This is realized by a continuous transition of an auxiliary parameter. In terms of phase field modeling this parameter is referred to as order parameter, whose governing equation is coupled to the mechanical problem. As phase field models for solidification simulations [14, 34] propose, the evolution of the order parameter is generally driven by the criterion of energy minimization. First phase field models for fracture as e.g. [15] or [23] were initially concerned with brittle fracture under quasi static monotonic loading. The total energy considered in these models accounts for the bulk energy and also for crack energy in the sense of Griffith's theory [7], which certainly represents a keystone of fracture mechanics. Besides the evolution governed by an energy criterion another pivotal benefit of these models is that no remeshing or refining algorithms are necessary as the crack field is incorporated by an additional degree of freedom. It evolves within the preexisting domain. Accordingly, the method was extended to the fields of cohesive fracture proposed in e.g. [16] and [33], ductile fracture proposed in e.g. [17] [22] and also models taking into account inertia for dynamic fracture [28]. Also an extension to fatigue crack initiation and growth was modeled by means of the phase field approach in [30, 29, 1, 31].

Another very important class of fracture problems, which will be treated within the present work, is concerned with materials that reveal a certain anisotropy of the resistance against fracture. In contrast to an elastic anisotropy of the material, which is mainly responsible for additional parameters in the stiffness tensor and accordingly effects the mechanical response to a certain load, the directionality of the fracture resistance has a crucial impact on the path a crack will follow through the material. This effect can be detected in experimental studies as performed in e.g. [11]. To incorporate this kind of anisotropic behavior within a phase field fracture model, a critical energy release rate depending on the crack deflection direction may be introduced. This approach, which generally resembles the Maximum Energy Release Rate (MERR) criterion [35], was introduced in terms of phase field modeling by Hakim and Karma [9] and also by Li et al. [19]. In the present work we study an alternative approach to modify the crack energy, that overcomes the issue of determining the crack tip orientation and therefore provides an appropriate framework for implicit monolithic solution schemes. In Section 2 we give a brief overview in terms of directional fracture resistance and illustrate potential causes. Subsequently the complete model is derived, where we start with the basic model proposed by Kuhn and Müller [15] and continue with the enhancement accounting for the anisotropy. Section 3 deals with the implementation of the model in a finite element framework, which was utilized for the computation of the examples presented in Section 4.

2 Phase field model for anisotropic fracture

2.1 Crack deflection in materials with directionality of the fracture resistance

One of the most important principles of todays understanding of fracture phenomena goes back to the early 20th century when Alan Arnold Griffith published his theory [7], which associates the change of surface energy with crack length. For an a priori known crack in a homogeneous, linear elastic and isotropic medium under quasi static loading he proposed the energy criterion

$$\mathcal{G}_c = \frac{\mathrm{d}\Gamma}{\mathrm{d}a} = -\frac{\mathrm{d}\Pi}{\mathrm{d}a} \tag{1}$$

for onset of crack extension. In Equation (1) Π is the potential energy stored in the structure under consideration and $\mathcal{G}_c$ is the materials critical surface energy density. The infinitesimal surface energy $\mathrm{d}\Gamma = \mathcal{G}_c \mathrm{d}a$ is proportional to the crack surface and accordingly Griffith's criterion states that crack growth occurs once the increase of surface energy balances the release of potential energy. Again, this criterion assumes a crack path, that is known a priori. However, different methods were proposed to determine the deflection direction for arbitrary plane loading, as for instance the principle of local symmetry [6] or the MERR criterion [35]. The latter states that assuming the energy release rate $\frac{\mathrm{d}\Gamma}{\mathrm{d}a}$ as a function of the potential direction of propagation, the crack will chose the direction maximizing the energy release. However, if the critical energy release rate $\mathcal{G}_c$ is also a function of the virtual deflection angle the MERR criterion is no more sufficient (see [20]). This special form of an anisotropy can have different sources. A typical example are thin walled structures manufactured by (hot-)rolling or extruding processes, as illustrated in Figure 1. These processes introduce a certain deformation of the microstructure of the metal products, which leads to an elongation of grains in a specific direction, as schematically shown by the microstructures on the bottom of Figure 1. The indicated crack paths illustrate transcrystalline crack growth for the left picture and intercrystalline crack growth for the right picture, respectively. Obviously, for an equal crack length a crack propagating through the material in vertical direction has to break through a higher number of grain boundaries than a crack propagating in horizontal direction. Analogous, in terms of intercrystalline crack extension the vertical crack has a much more tortuous path over an equal length than the horizontal crack. Thus, to obtain a crack growing purely vertical, a higher force magnitude is expected than for a crack growing purely horizontally. In other terms, the resistance against cracking, which is referred to as fracture toughness, varies with the virtual crack direction. Accordingly, not only the loading quantity $\frac{\mathrm{d}\Pi}{\mathrm{d}a}$ depends on the direction but also the material parameter $\mathcal{G}_c$. An approach [13] to include such an anisotropy in the determination of the crack growth direction suggests to consider the ratio of these quantities and specify the maximum of this function of the potential crack extension angle. An elliptical interpolation is used for the quantity $\mathcal{G}_c$ with respect to the virtual cracking direction.

2.2 Phase field model for materials with directional fracture resistance

Within a large variety of physical processes different microstructures or phase compositions are generated. For example the kinetics of martensite to austenite transformation in a certain alloy. The process of solidification in metal casting as well as the cracking behavior can be modeled by a phase field. In fracture the phases are associated with broken and intact material. The tracking of an interface is problematic from an numerical perspective.

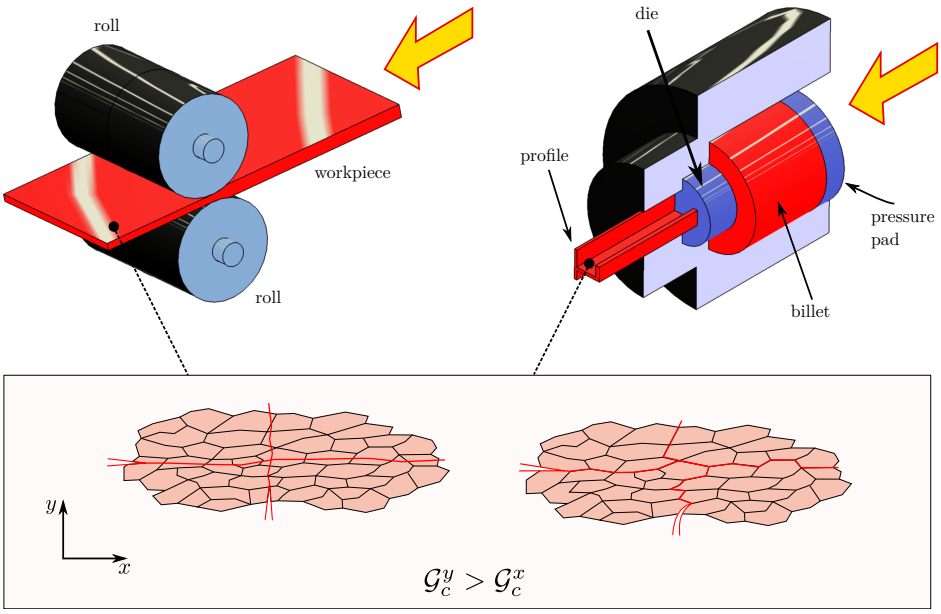

Figure 1 Illustration of two manufacturing processes (left: rolling, right: extruding) for thin walled structures and schematic illustration of microstructure with two crack paths indicated (left: transcrystalline crack propagation, right: intercrystalline crack propagation).

Especially, sharp interface models frequently encounter problems (see. e.g. [26, 25]). In terms of fracture, the nature of this issue often lies in the discretization, which is explicitly mapped to the crack surface. As an alternative, the framework of phase field modeling provides a method overcoming a number of issues of sharp interface models. Within this method an auxiliary parameter, commonly referred to as order parameter or phase field parameter, is introduced to indicated the phase at a certain location. Within the following fracture model the order parameter is $s(\mathbf{x}, t)$ and it takes the value $s = 1$ as long as the material is completely intact. Fully broken material is then indicate by $s = 0$. The transition between these values is diffuse, which conveniently overcomes the issue of discontinuities. The following sections explain in detail, how the coupling of this additional field to the deformation is done and how the evolution of the phase field $s(\mathbf{x}, t)$ is described.

2.2.1 Phase field model for brittle fracture

Within material science the evolution of the phase are commonly derived from potentials of the free energy, which mathematically are treated as functionals $F[s(\mathbf{x}, t)]$. The temporal evolution of the phase field variable, which is governed by nonlinear partial differential equations can be obtained by

$$\frac{\partial s(\mathbf{x}, t)}{\partial t} = -M \frac{\delta F}{\delta s(\mathbf{x}, t)}, \tag{2}$$

which is referred to as the time dependent Ginzburg-Landau equation and was first applied to first order phase transformations in [4]. In this equation M is a viscous regularization coefficient to control the relaxation towards stationary states. The characteristic energy

potential ψ depends on a combination of bulk energy and an interface energy such that

$$F\left[s(\mathbf{x},t)\right] = \int_{\Omega} \psi(s, \nabla s)\, \mathrm{d}V = \int_{\Omega} f(s) + \frac{1}{2}\kappa|\nabla s|^2 \, \mathrm{d}\Omega. \tag{3}$$

In this equation $f(s)$ represents the bulk energy density and a nonlocal contribution in form of a gradient term accounts for interfacial energy. The coefficient κ associated with the gradient energy term must be positive to ensure stability of one phase states. Using the free energy Equation (3) and applying the formal variation of the functional $F\left[s(\mathbf{x},t)\right]$, namely

$$\delta F\left[s(\mathbf{x},t)\right] = \int_{\Omega} \delta s \left[\frac{\partial \psi}{\partial s} - \nabla \cdot \left(\frac{\partial \psi}{\partial \nabla s}\right)\right] \, \mathrm{d}\Omega \tag{4}$$

with δs being variation of s the functional derivative can be formulated by

$$\frac{\delta F}{\delta s} = \frac{\partial \psi}{\partial s} - \nabla \cdot \left(\frac{\partial \psi}{\partial \nabla s}\right) \tag{5}$$

and Equation (2) yields

$$\frac{1}{M}\dot{s} = \nabla \cdot \left(\frac{\partial \psi}{\partial \nabla s}\right) - \frac{\partial \psi}{\partial s}. \tag{6}$$

The state $\delta F/\delta s = 0$ is a necessary condition for an extreme value of $s(\mathbf{x},t)$ and hence characterizes stationary states. Accordingly, Equation (6) can be viewed as relaxation to reach stationary states governed by the viscosity parameter $M > 0$.

In order to develop a phase field model for brittle fracture, Kuhn and Müller [15] utilized the energy potential

$$F[\boldsymbol{\varepsilon}(\mathbf{u},t), s(\mathbf{x},t)] = \int_{\Omega} \Bigg[\underbrace{(g(s)+\eta)\frac{1}{2}\boldsymbol{\varepsilon} : [\mathbb{C}\boldsymbol{\varepsilon}]}_{\psi_e} + \underbrace{\mathcal{G}_c \left(\frac{(1-s)^2}{4\epsilon} + \epsilon|\nabla s|^2 \right)}_{\psi_c} \Bigg] \mathrm{d}V, \tag{7}$$

which was proposed in [3, 2] as a regularization of the variational formulation of brittle fracture developed by Francfort and Marigo in [21]. The two contributions in Equation (7), ψ_e and ψ_c represent energies related to deformation and cracking, respectively. The first term ψ_e is the elastic energy density for small deformations with the linearized second order strain tensor $\boldsymbol{\varepsilon}$ and the isotropic fourth order stiffness tensor $\mathbb{C}$. The second term in Equation (7) may be interpreted as regularization of Griffith's surface energy. The parameter ϵ controls the width of the transition zone between the phases and can therefore be considered a regularization parameter. The multiplication of the strain energy with $g(s) + \eta$ accounts for the degradation of the stiffness in areas with $1 > s$. In this regard $g(s)$ is referred to as a degradation function modeling the material response as a variation of the phase field s. The least set of requirements for this functions is $g(s = 0) = 0$, $g(s = 1) = 1$ and $g'(s = 0) = 0$. The parameter η with $0 < \eta \ll 1$ ensures a residual stiffness $\eta\mathbb{C}$ for numerical convenience. Within Figure 2 the described approximation scheme for the fracture problem by means of the introduced phase field framework is illustrated. The crack potential ψ_c of Equation (7) consists of a nonlocal part characterized by the spatial gradient of s and a local part, characterized by the monotonous function $(1-s)^2$. This local contribution has crucial impact on the model properties (see e.g. [18]). In contrast, the double well function, which

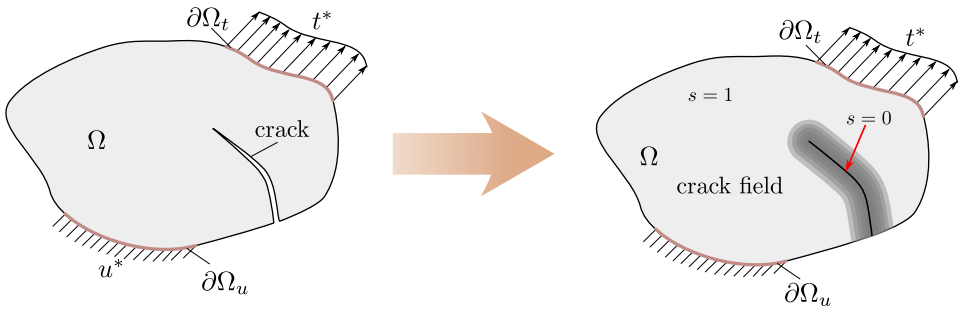

sharp interface representation diffuse representation

Figure 2 Schematic illustration of approximation of fracture problem by means of phase field modeling: left, body with real sharp crack; right, diffuse representation of crack introducing a continuous crack field.

was applied in e.g. [12] in terms of fracture reveals a kind of naturally induced barrier between two phases. Irreversibility of the fracture process is accordingly not generally ensured by this monotonous potential. This quadratic potential, however, provides several crucial benefits, such as that the mathematical property of Γ-convergence (see. e.g. [5]) can be proven for Equation (7). Further the corresponding states of the potential for the opposite phases $s = 1$ and $s = 0$ yield the maximum distance within the relevant range $[0, 1]$ leading to a distinct separation between intact and broken material with regard to the potential energy, which prevents the crack field from growing fat. The stresses can be derived from the potential ψ by

$$\boldsymbol{\sigma} = \frac{\partial \psi}{\partial \boldsymbol{\varepsilon}} = (g(s) + \eta)\mathbb{C}\boldsymbol{\varepsilon}, \tag{8}$$

in which a hyperelastic material behavior is presumed. With Equation (7) a proper energy potential depicting a potentially fractured body is given and an evolution of $s(\mathbf{x}, t)$ with respect to time can be formulated considering the general law for phase transformation of Equation (6), which yields a Ginzburg-Landau type evolution equation

$$\dot{s} = -M\frac{\delta}{\delta s}(\psi_e + \psi_c) = -M\left\{\frac{1}{2}g'(s)\boldsymbol{\varepsilon} : [\mathbb{C}\boldsymbol{\varepsilon}] - \mathcal{G}_c\left(\frac{1-s}{2\epsilon} + 2\epsilon\nabla\cdot\nabla s\right)\right\}. \tag{9}$$

With the kinetic parameter M approaching infinity, quasi static conditions are approximated. Furthermore, this evolution equation points out the significance of the condition $g'(s = 0) = 0$ as without such a constraint the evolution of s would still continue even for broken material.

2.2.2 Incorporation of fracture toughness anisotropy

The model above predicts the crack pattern, that minimizes the total internal energy. The evolution can be interpreted as a competition between strain energy and crack energy at any time. The latter is not dependent on the potential extension direction within the original formulation [15] of brittle fracture. As stated above, a common way to incorporate directionality of the fracture resistance is to assume the critical energy release rate $\mathcal{G}_c$ as a function of the virtual crack growth direction. Declaring φ the angle between crack growth direction and a specified axis this yields $\mathcal{G}_c = \mathcal{G}_c(\varphi)$. In the context of phase field modeling this approach was studied in [9] and [19]. In this regard, the crack orientation must be

determined as the normal vector

$$\mathbf{n} = \frac{\nabla s}{|\nabla s|} \tag{10}$$

of the crack trajectory as direction for the critical energy release rate $\mathcal{G}_c(\mathbf{n})$. This definition is problematic at areas where ∇s vanishes, which renders Equation (10) impractical.
As an alternative approach $\mathcal{G}_c$ may be kept constant and instead the nonlocal part of the crack energy density $\psi_c^{\mathrm{nl}} = \mathcal{G}_c \epsilon |\nabla s|^2$ is modified in order introduce directionality. This is induced by a proper weighting of the particular components of the gradient. Visualizing the unmodified nonlocal crack potential for the 2d case in a proper axis system one obtains a paraboloidal (left illustration in Figure 3). This indicates that the direction of ∇s has no effect on the crack energy in the isotropic formulation. In contrast, if the paraboloid is deformed towards an elliptical shape, the direction of ∇s will indeed affect the total energy. For instance a gradient with a high $\frac{\partial s}{\partial x}$ contribution will shift ψ_c^{nl} to a higher level compared to a gradient with a high $\frac{\partial s}{\partial y}$ contribution with equal magnitude. Such a transformation of the nonlocal crack potential can be accomplished by substituting the identity tensor in

$$|\nabla s|^2 = \nabla s^T \mathbf{1} \nabla s \tag{11}$$

by an appropriate second order tensor $\mathbf{\Phi}$ such that the new total energy is obtained with the crack energy density taking into account the crack direction by means of the crack fields gradient with

$$\psi_c = \mathcal{G}_c \left[\frac{(1-s)^2}{4\epsilon} + \epsilon \left(\left(\frac{\partial s}{\partial x} \right)^2 \Phi_{11} + \frac{\partial s}{\partial x} \frac{\partial s}{\partial y} \Phi_{12} + \left(\frac{\partial s}{\partial y} \right)^2 \Phi_{22} \right) \right] \tag{12}$$

within a plane setting. The tensor $\mathbf{\Phi}$ may be referred to as resistance tensor and for the simplest case accounting for a modification illustrated in Figure 3 this tensor takes the diagonal form

$$\mathbf{\Phi}_0 = \begin{pmatrix} 1+\alpha & 0 \\ 0 & 1-\alpha \end{pmatrix} \tag{13}$$

with the respective eigenvalues $1 \pm \alpha$ quantifying the degree of directionality governed by the parameter α. This formulation represents an elliptical interpolation between the values $1+\alpha$ and $1-\alpha$ with the respective reference axis represented by the eigenvectors. Suppose, the principal axes deviate from the reference system, then $\mathbf{\Phi}$ may be rotated via the rotation tensor $\mathbf{R}(\theta)$ to obtain

$$\mathbf{\Phi} = \mathbf{R}\mathbf{\Phi}_0\mathbf{R}^T = \begin{pmatrix} 1+\alpha\left(\cos^2\theta - \sin^2\theta\right) & 2\alpha \sin\theta\cos\theta \\ 2\alpha\sin\theta\cos\theta & 1-\alpha\left(\cos^2\theta - \sin^2\theta\right) \end{pmatrix}. \tag{14}$$

Incorporating this formulation of the resistance tensor in the energy functional Equation (7) yields the evolution equation of the phase field model for brittle fracture for materials with anisotropic fracture toughness

$$\dot{s} = -M \left\{ \frac{1}{2} g'(s) \boldsymbol{\varepsilon} : [\mathbb{C}\boldsymbol{\varepsilon}] - \mathcal{G}_c \left(\frac{1-s}{2\epsilon} + 2\epsilon \nabla \cdot (\mathbf{\Phi} \nabla s) \right) \right\}, \tag{15}$$

where now the orientation dependency is characterized by material parameters α and θ representing the intensity and orientation of the anisotropy, respectively. This characterization

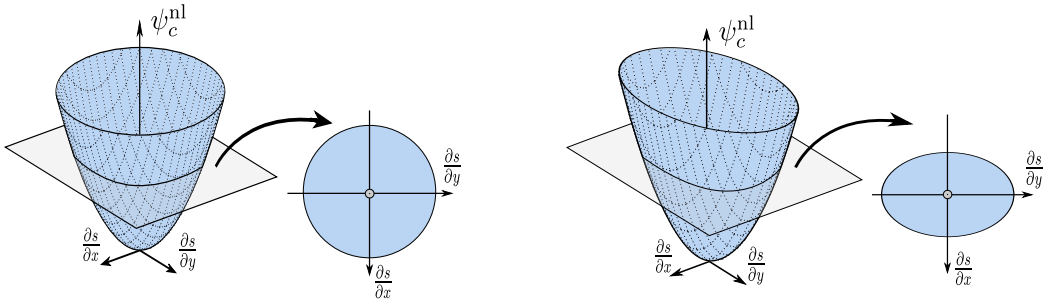

no favored direction of gradient directionality

Figure 3 Schematic illustration of nonlocal crack potential assuming plane crack evolution of the original formulation (paraboloid in $\frac{\partial s}{\partial x}, \frac{\partial s}{\partial y}$-system) and modified formulation (elliptic paraboloid in $\frac{\partial s}{\partial x}, \frac{\partial s}{\partial y}$-system).

resembles the kind of a so-called twofold anisotropy. However implementing more general forms of the resistance tensor, the model could also account for more complex anisotropies as outlined in e.g. [19, 32].

The phase field evolution Equations (9) and (15) have the form of a inhomogeneous second order partial differential equation, which can be solved analytically only for a number of special cases. For the one dimensional case as depicted in Figure 4, Equation (15) with Equation (13) becomes

$$0 = 2(1+\alpha)\epsilon \frac{\mathrm{d}^2 s}{\mathrm{d}x^2} - \frac{s-1}{2\epsilon} \tag{16}$$

if a preexisting crack within an unloaded domain is presumed. This differential equation can be solved utilizing exponential trial functions and presuming the boundary conditions $s'(1) = s'(-1) = 0$ and $s(0) = 0$ one obtains the phase field

$$s(x) = 1 - \exp\left(\frac{-|x|}{2\epsilon\sqrt{1+\alpha}}\right). \tag{17}$$

Accordingly the shape of $s(x)$ does not solely depend on the length scale ϵ but also on the parameter α. As will be outlined in Section 4.1, the one dimensional solution can be extended in order to approximate an unidirectional crack in two dimensions. This solution is illustrated in Figure 4. The solid lines correspond to the equation of the original model [15] for isotropic materials for two different values of ϵ, where the crack becomes more narrow for a smaller ϵ. The dashed lines in contrast are obtained by Equation (17) with equal ϵ but different values for α. These plots reveal a crucial property of the modification. Assuming a basic resistance tensor of the form of Equation (13) the parameter α yields a variation of the actual length scale with the consequence of a wider crack for $\alpha > 0$ and a sharper crack for $\alpha < 0$. As the quality of the approximation of cracks by a phase field model depends on the regularization length, the intensity parameter α may therefore be chosen as little as possible relatively to ϵ. Note that the modification yields the original model for the case of zero anisotropy, namely $\alpha \to 0$.

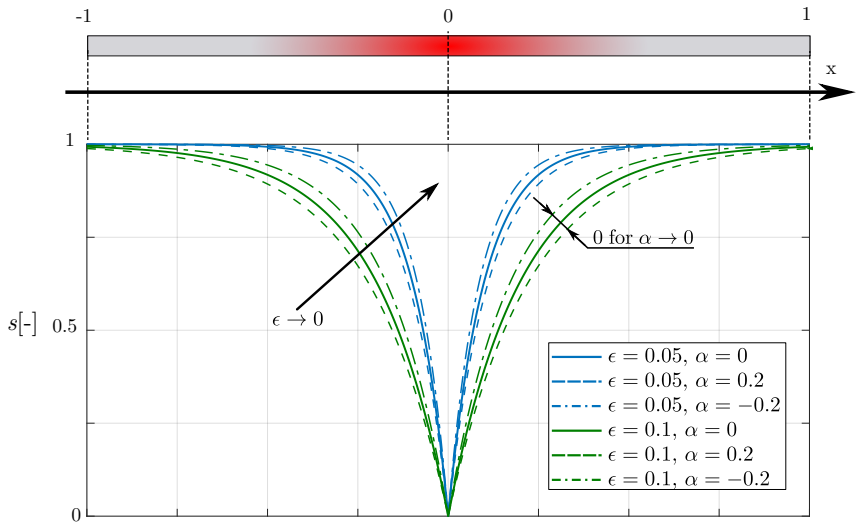

Figure 4 Illustration of the analytic solution of the proposed phase field model within one dimensional assessment of a stationary crack using different values for parameters ϵ and α.

3 Numerical implementation

The phase field model for materials with anisotropic fracture toughness derived in the previous sections is discretized and implemented into a finite element framework. With the evolution equation for the phase field Equation (15), the set of partial differential equations governing the displacements $\mathbf{u}$ and the order parameter s is

$$\begin{aligned} \mathbf{0} &= \operatorname{div} \boldsymbol{\sigma} \\ \frac{\mathcal{G}_c}{2\epsilon} &= \frac{\dot{s}}{M} + \frac{1}{2} g(s)' \boldsymbol{\varepsilon} : \mathbb{C}\boldsymbol{\varepsilon} + s\frac{\mathcal{G}_c}{2\epsilon} - \mathcal{G}_c 2\epsilon \nabla \cdot (\boldsymbol{\Phi} \nabla s)\,, \end{aligned} \tag{18}$$

neglecting volume forces in the mechanical equilibrium. The respective weak forms of these equations can be obtained by multiplying both equations with virtual quantities $\delta\mathbf{u}$ and δs, respectively. This yields

$$0 = -\int_{\Omega} \boldsymbol{\sigma} : \delta\boldsymbol{\varepsilon} \, \mathrm{d}V + \int_{\partial\Omega_t} \delta\mathbf{u} \cdot \mathbf{t}^* \, \mathrm{d}S \tag{19}$$

with vector $\mathbf{t}^*$ of prescribed tractions that act on the boundary $\partial\Omega_t$ and

$$0 = -\int_{\Omega} \left[\delta s \left(\frac{\dot{s}}{M} + \frac{1}{2} g(s)' \boldsymbol{\varepsilon} : \mathbb{C}\boldsymbol{\varepsilon} + (s-1)\frac{\mathcal{G}_c}{2\epsilon} \right) + \mathcal{G}_c 2\epsilon \nabla \delta s \cdot \boldsymbol{\Phi} \nabla s \right] \mathrm{d}V, \tag{20}$$

where integration by parts was applied. For the derivations in the following a 2d setting is presumed and Voigt's notation for symmetric tensors is applied. The field quantities $\mathbf{u}$ and s are discretized elementwise using shape functions N_I with $I = 1, \ldots, n$ and n the number of nodes per element. Accordingly,

$$\mathbf{u}(\mathbf{x}) = \sum_{I=1}^{n} N_I(\mathbf{x}) \mathbf{u}_I \qquad \text{and} \quad s(\mathbf{x}) = \sum_{I=1}^{n} N_I(\mathbf{x}) s_I, \tag{21}$$

with nodal quantities $\mathbf{u}_I$ and s_I. An analog discretization using the same shape functions N_I is applied for virtual quantities. Further, the strain tensor $\boldsymbol{\varepsilon}$ as well as the spatial gradient ∇s are discretized by

$$\varepsilon(\mathbf{x}) = \sum_{I=1}^{n} \boldsymbol{B}_I^{\mathbf{u}}(\mathbf{x})\mathbf{u}_I \qquad \text{and} \quad \nabla s(\mathbf{x}) = \sum_{I=1}^{n} \boldsymbol{B}_I^{s}(\mathbf{x})s_I, \tag{22}$$

using the respective operator matrices

$$\boldsymbol{B}_I^{\mathbf{u}}(\mathbf{x}) = \begin{bmatrix} N(\mathbf{x})_{I,x} & 0 \\ 0 & N(\mathbf{x})_{I,y} \\ N(\mathbf{x})_{I,y} & N(\mathbf{x})_{I,x} \end{bmatrix} \qquad \text{and} \quad \boldsymbol{B}_I^{s} = \begin{bmatrix} N(\mathbf{x})_{I,x} \\ N(\mathbf{x})_{I,y} \end{bmatrix}. \tag{23}$$

The vector of the internal forces, which corresponds to the displacements $\mathbf{u}$ and s at the particular node I are derived from Equations (19) and (20) as

$$\boldsymbol{F}_I^{\mathbf{u}} = \int_{\Omega} \left(\boldsymbol{B}_I^{\mathbf{u}}\right)^T \boldsymbol{\sigma} \, \mathrm{d}V \tag{24}$$

and

$$F_I^{s} = \int_{\Omega} \left[N_I \left(\frac{\dot{s}}{M} + \frac{1}{2} g(s)' \boldsymbol{\varepsilon}^T \mathbb{C} \boldsymbol{\varepsilon} + \mathcal{G}_c \frac{s-1}{2\epsilon} \right) + 2\mathcal{G}_c \epsilon \left(\boldsymbol{B}_I^{s}\right)^T \boldsymbol{\Phi} \nabla s \right] \mathrm{d}V. \tag{25}$$

The Newton-Raphson scheme is applied to solve the nonlinear system. This requires the tangential stiffness matrix associated to the framework. These particular components are obtained by derivation of the residual with respect to the unknown field quantities as

$$\boldsymbol{K}_{IJ}^{\mathbf{uu}} = \frac{\partial \boldsymbol{F}_I^{\mathbf{u}}}{\partial \mathbf{u}_J} = \int_{\Omega} \boldsymbol{B}_I^{\mathbf{u}} (g(s) + \eta) \mathbb{C} \boldsymbol{B}_J^{\mathbf{u}} \, \mathrm{d}V, \tag{26}$$

$$\boldsymbol{K}_{IJ}^{s\mathbf{u}} = \frac{\partial \boldsymbol{F}_I^{s}}{\partial \mathbf{u}_J} = \int_{\Omega} N_I g(s)' \left(\mathbb{C}\boldsymbol{\varepsilon}\right)^T \boldsymbol{B}_J^{\mathbf{u}} \, \mathrm{d}V, \tag{27}$$

$$\boldsymbol{K}_{IJ}^{\mathbf{u}s} = \frac{\partial \boldsymbol{F}_I^{\mathbf{u}}}{\partial s_J} = \int_{\Omega} \left(\boldsymbol{B}_I^{\mathbf{u}}\right)^T g(s)' \mathbb{C}\boldsymbol{\varepsilon} N_J \, \mathrm{d}V, \tag{28}$$

$$\boldsymbol{K}_{IJ}^{ss} = \frac{\partial \boldsymbol{F}_I^{s}}{\partial s_J} = \int_{\Omega} \left[N_I N_J \left(\frac{1}{2} g(s)' \boldsymbol{\varepsilon}^T \mathbb{C} \boldsymbol{\varepsilon} + \frac{G_c}{2\epsilon} \right) + 2\mathcal{G}_c \epsilon \left(\boldsymbol{B}_I^{s}\right)^T \boldsymbol{\Phi} \boldsymbol{B}_J^{s} \right] \mathrm{d}V \tag{29}$$

Finally, the damping matrix can be derived which reveals zero contributions except for the component

$$D_{IJ}^{s\dot{s}} = \frac{\partial F_I^{s}}{\partial \dot{s}} = \int_{\Omega} \frac{N_I N_J}{M} \, \mathrm{d}V. \tag{30}$$

The implicit Euler method is applied for the transient problem. To ensure a reliable convergence behavior, automatic step size adjustment is applied to ensure a stable computation even for situations of a rapid evolution of the crack field.

4 Numerical examples

The phase field model derived in the previous sections was implemented into a user routine for a quadrilateral element of the software FEAP 8.4. This routine was used for the simulations outlined in the following.

4.1 Energetic assessment of the modification

An general solution of the partial differential equation Equation (15) can not be obtained. However, for an unidirectional crack one can presume that there is no variation of the phase field with respect to the direction of crack extension and accordingly one may approximate the 2d solution by an extrusion of the one dimensional solution Equation (16). As illustrated in Figure 5a) the diffuse region at the and of the crack is neglected within this approximation. However, this does not effect the following energy assessment as it can be shown that the crack energy for this part vanishes for $\epsilon \to 0$. Considering a stationary crack in an anisotropic material as it may be characterized by Equation (13), extending solely in one coordinate direction (see Figure 5b)), the energy consumed by this crack can be approximated using Equation (17) with

$$E_c = \int_{-a/2}^{a/2} \int_{-L}^{L} \psi_c \, \mathrm{d}x\mathrm{d}y = a\mathcal{G}_c\sqrt{1+\alpha}\left[1 - \exp\left(\frac{-L}{\epsilon\sqrt{1+\alpha}}\right)\right]. \tag{31}$$

Presuming a very fine regularization ($\epsilon \to 0$) for a crack of length one this expression simplifies to

$$E_c = a\mathcal{G}_c\sqrt{1+\alpha} \qquad \text{for } \epsilon \to 0 \tag{32}$$

Note that this derivation can be repeated for a crack under the same assumptions but extending purely in orthogonal direction. The respective surface energy would then be obtained as $E_c = a\mathcal{G}_c\sqrt{1-\alpha}$.

In order to prove the accuracy, these approximations may be verified by means of respective 2d simulations with the proposed phase field model. The set up for this stationary simulation is indicated in Figure 5b). Due to the symmetry of the problem with respect

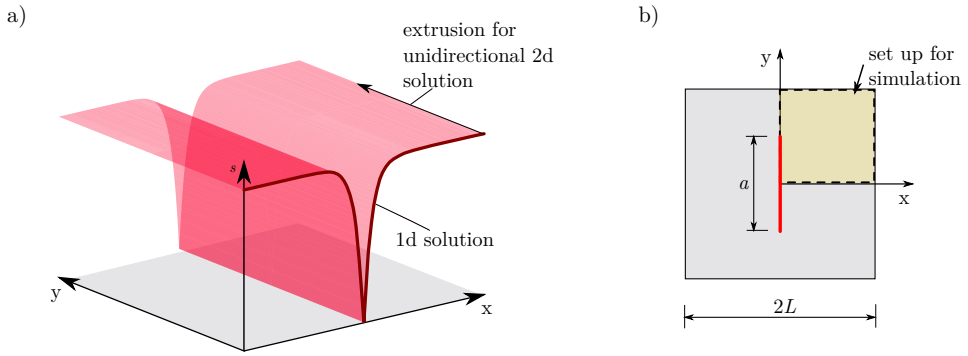

Figure 5 Schematic illustration of the extension of the one dimensional phase field solution to an unidirectional crack: a) segment of surface plot of the crack field; b) set up for stationary simulations.

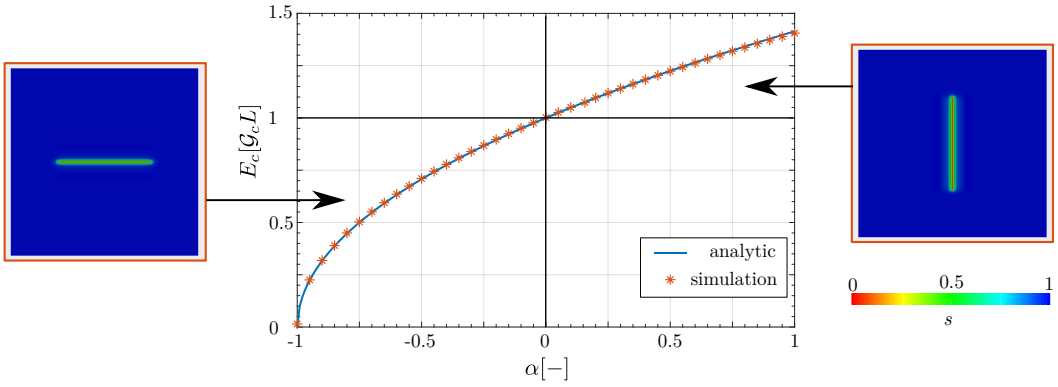

Figure 6 Comparision of analytic energy estimate of anisotropic model with results obtained from stationary finite element simulations.

to the x and y axes only a quarter of the domain was discretized using 12544 nodes. The mesh was refined in the region containing the crack in order to obtain an accurate solution of the crack field and to enable for small values of the length scale ϵ. Several simulations where run using different values of α in the range $-1 \leq \alpha \leq 1$, where simulations with $\alpha > 0$ represent cracks extending in y-direction and $\alpha < 0$ represent crack extending in x-direction. The crack energy was numerically integrated in the domain and multiplied by the factor 4. A comparison of the theoretical estimate of the total crack energy with the energy obtained by the simulations is shown in Figure 6. It shows agreement of the analytic solution with the simulation results. Therefore, it illustrates the effect of the proposed modification in terms of an energetic view.

4.2 Plate with sharp notch

The aim of this example is to illustrate the abilities of the developed model with regard to predicting crack paths. The resistance tensor $\mathbf{\Phi}$ entering the evolution equation of the phase field incorporates the two parameters α and θ. These parameters are supposed to quantify the intensity and direction of the anisotropy of the fracture resistance. In order to illustrate the sensitivity of the model to a parameter variation, a notched plate was set up. The set up is depicted in Figure 7. In all simulations, displacements were blocked in vertical direction for

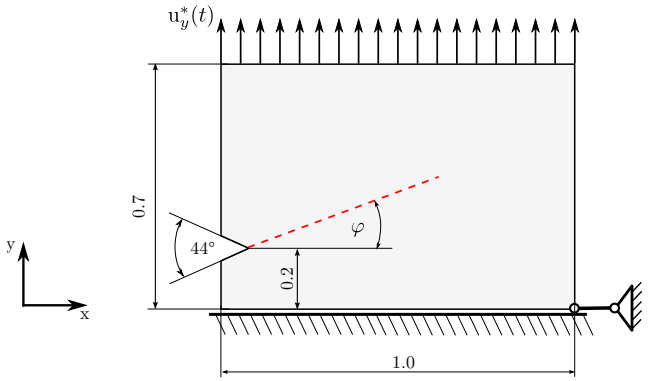

Figure 7 Illustration of set up for phase field simulation of a plate with notch.

nodes of the lower boundary edge and in horizontal direction for the node at the lower right corner of the plate. A spatially constant displacement load $u_y^*(t)$ was applied for the top edge nodes as monotonically increasing function. The specimen was discretized by means of 14899 nodes and 14406 elements with almost equal edge length. The length scale was kept constant for all simulations at a value of $\epsilon = 0.015$. For this particular set up, cracks will initiate at the notch tip. The initial deviation of the crack from a pure horizontal path, is quantified by the angle φ as indicated in Figure 7. The results for several simulations are illustrated in Figure 8. This comparison clearly indicates that both parameters have significant effect on the crack growth direction. The upper left contour plot shows a horizontal crack path, which is expected for the applied displacement load with both parameters set to zero. In contrast if α or θ are increased the crack paths reveal a deflection angle φ. For a constant orientation θ this deflection angle increases with increasing the value of intensity α.

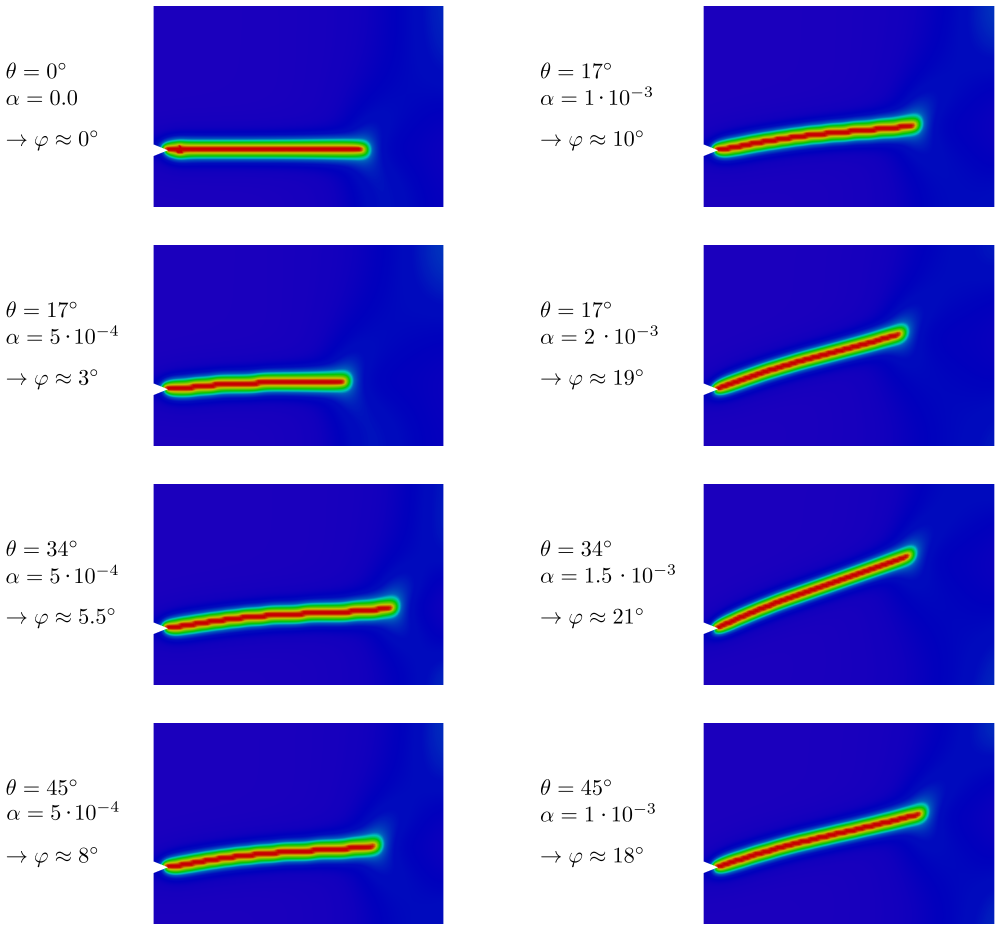

Figure 8 Comparison of deflection angle of crack paths for different parameter sets obtained from FEM simulations with the proposed anisotropic fracture model.

4.3 Plate with hole

The numerical example outlined in the following was set up in order to verify the practical usage of the modified phase field model. In the focus is an assessment of the model with respect to experimental findings from a study done by Judt et al. [11]. Plates of rolled

aluminum sheets where subjected to tensile testes. The aluminum raw material revealed a twofold anisotropy as described within the previous section. The geometry of the specimens is depicted in Figure 9a), which also illustrates the set up for the phase field simulations. The anisotropy of the plates was determined with respect to the indicated x-y-system. Accordingly, the resistance tensor reveals a structure as in Equation (13). Phase field simulations with a monotonously increasing displacement load in positive y direction where performed for different parameterizations of α. The results are illustrated in Figure 9 by the three contour

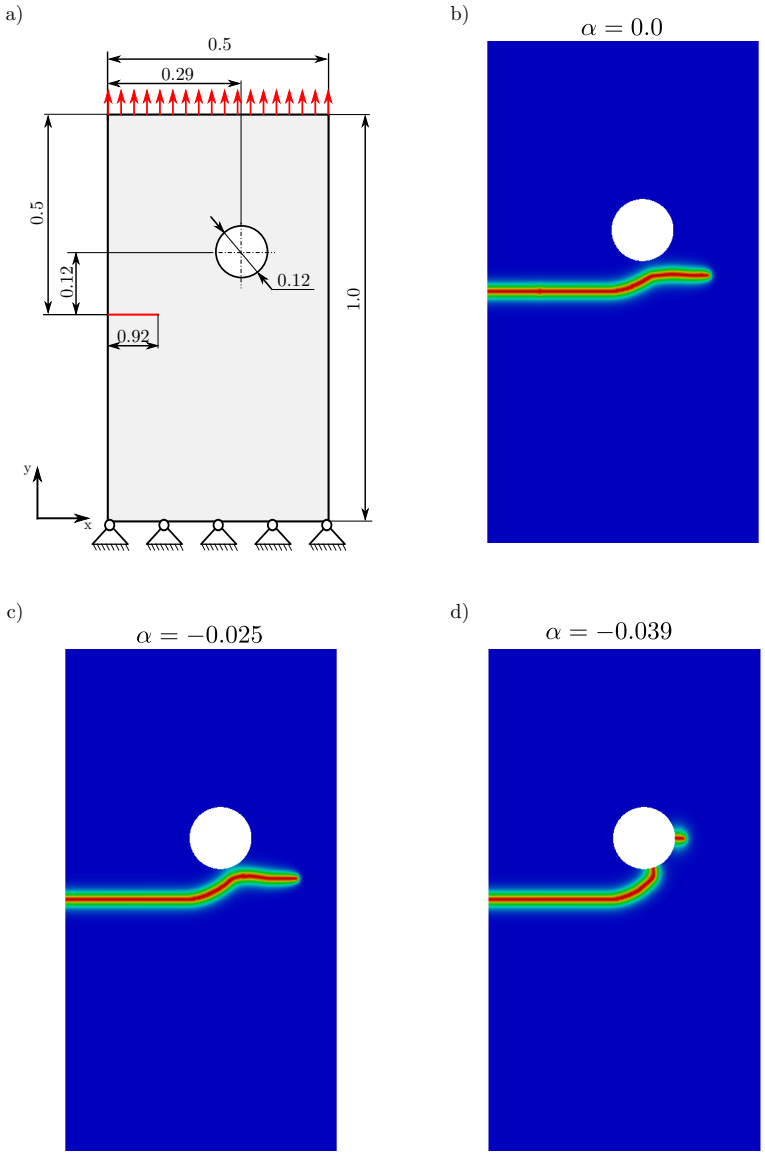

Figure 9 Set up and results (contour plots of phase field variable s) from phase field simulations with different values for α: b) $\alpha = 0.0$, c) $\alpha = -0.025$, d)$\alpha = -0.039$.

plots of the phase field variable s. The plot Figure 9d) shows the crack path obtained by the simulation with the highest magnitude for α. This crack path is quiet similar to the crack path found in [11] by experiments. As the contour plots Figure 9b) and c) show, the phase field model predicts that the induced crack passes the hole instead of growing into it. This is

due to the lower magnitude of the anisotropy, which then favors the y direction less for crack extension. Note that the crack predicted by the simulation with $\alpha = -0.025$ lies between the other two cases. Further the crack patterns shown in Figure 9b) and c) correlate with the crack paths found in [11] by a conventional crack simulation technique.

5 Concluding remarks

A phase field fracture model has been presented, which is able to account for an anisotropic fracture resistance. The anisotropy influences the path of a crack growing through the material. The nonlocal part of the regularized crack energy density is modified in order to enhance the isotropic phase field model for brittle fracture. As the evolution is governed by energy minimization, the weighting of the respective components of the spatial gradient of the order parameter includes the directionality regarding crack growth. The characteristic of the anisotropy is quantified by two additional parameters within the governing equations of the model. By means of analytic considerations it is explained how the modification effects the crack energy with respect to the parameterization. Comparing these derivations with numerical results a good agreement is confirmed. Further simulations show that cracks tend to grow in the direction favored by the parameterization. Good agreement with experimental results is also obtained for simulated crack patterns in holed plates. Accordingly, the approach we follow within this contribution seems to provide a sound basis for even more complex anisotropies. With regard to further investigations the introduced resistance tensor may be modified in order to represent materials with more complex polar plots of the critical energy release rate (see e.g. [19, 27]).

References

1 R. Alessi, S. Vidoli, and L. DeLorenzis. A phenomenological approach to fatigue with a variational phase-field model: The one-dimensional case. *Engineering Fracture Mechanics*, 190:53–73, 2017.

2 B. Bourdin. Numerical implementation of the variational formulation of brittle fracture. *Interfaces and Free Boundaries - INTERFACE FREE BOUND*, 9:411–430, 2007.

3 B. Bourdin, G. A. Francfort, and J-J. Marigio. Numerical experiments in revisited brittle fracture. *Journal of the Mechanics and Physics of Solids*, 48:797–826, 2000.

4 S. Chan. Steady-state kinetics of diffusionless first order phase transformation. *The Journal of Chemical Physics*, 67(12):5755–5762, 1977.

5 E. De Giorgi and G. Dal Maso. Γ-convergence and calculus of variations. In *Mathematical Theories of Optimization*, pages 121–143, Berlin, Heidelberg, 1983. Springer.

6 Robert V. Goldstein and Rafael L. Salganik. Brittle fracture of solids with arbitrary cracks. *International Journal of Fracture*, 10:507–523, 1974.

7 A. A. Griffith. The phenomena of rupture and flow in solids. *Philosophical Transactions of the Royal Society of London*, 221:163–198, 1921.

8 D. Gross and Th. Seelig. *Bruchmechanik–Mit einer Einfürung in dei Mikromechanik*. Springer, Heidelberg, 5 edition, 2011.

9 V. Hakim and A. Karma. Laws of crack motion and phase-field models of fracture. *Journal of the Mechanics and Physics of Solids*, 57(2):342–368, 2009.

10 P. O. Judt and A. Ricoeur. Crack growth simulation of multiple cracks systems applying remote contour interaction integrals. *Theoretical and Applied Fracture Mechanics*, 75:78–88, 2015.

11 P. O. Judt, A. Ricoeur, and G. Linek. Crack path prediction in rolled aluminum plates with fracture toughness orthotropy and experimental validation. *Engineering Fracture Mechanics*, 138:33–48, 2015.

12 A. Karma, D. Kessler, and H. Levine. Phase-field model of mode iii dynamic fracture. *Physical Review Letters*, 87:045501, 2001.

13 A.P. Kfouri. Crack extension under mixed-mode loading in an anisotropic mode-asymmetric material in respect of resistance to fracture. *Fatigue and Fracture of Engineering Materials and Structures*, 19(1):27–38, 1996.

14 Ryo Kobayashi. Modeling and numerical simulations of dendritic crystal growth. *Physica D: Nonlinear Phenomena*, 63(3):410–423, 1993.

15 C. Kuhn and R. Müller. A continuum phase field model for fracture. *Engineering Fracture Mechanics*, 77:3625–3634, 2010.

16 C. Kuhn and R. Müller. A discussion of fracture mechanisms in heterogeneous materials by means of configurational forces in a phase field fracture model. *Computer Methods in Applied Mechanics and Engineering*, 312:95–116, 2016.

17 C. Kuhn, T. Noll, and R. Müller. On phase field modeling of ductile fracture. *GAMM Mitteilungen*, 39:35–54, 2016.

18 C. Kuhn, A. Schlüter, and R. Müller. On degradation functions in phase field fracture models. *Computational Materials Science*, 108:374–384, 2015.

19 B. Li, C. Peco, D. Millán, I. Arias, and M. Arroyo. Phase-field modeling and simulation of fracture in brittle materials with strongly anisotropic surface energy. *International Journal for Numerical Methods in Engineering*, 102(3-4):711–727, 2015.

20 L. Ma and A. Korsunsky. On the use of vector j-integral in crack growth criteria for brittle solids. *International Journal of Fracture*, 133, 2005.

21 J. J. Marigo. Modelling of brittle and fatigue damage for elastic material by growth of microvoids. *Engineering Fracture Mechanics*, 21:861–874, 1985.

22 C. Miehe, F. Aldakheel, and T Stephan. Phase-field modeling of ductile fracture at finite strains. a robust variational-based numerical implementation of a gradient-extended theory by micromorphic regularization: Phase field modeling of ductile fracture. *International Journal for Numerical Methods in Engineering*, December 2016. doi:10.1002/nme.5484.

23 C. Miehe, F. Welschinger, and M. Hofacker. Thermodynamically consistent phase-field models of fracture: Variational principles and multi-field fe implementations. *International Journal for Numerical Methods in Engineering*, 83(10):1273–1311, 2010.

24 P. O'Hara, J. Hollkamp, C.A. Duarte, and T. Eason. A two-scale generalized finite element method for fatigue crack propagation simulations utilizing a fixed, coarse hexahedral mesh. *Computational Mechanics*, 57:55–74, 2016.

25 N. Provatas and K. Elder. *Phase Field Methodes in Material Science and Engineering*. Wiley, Berlin, 1 edition, 2010.

26 A.H. Rajkotwala, A. Panda, E.A.J.F. Peters, M.W. Baltussen, C.W.M. [van der Geld], J.G.M. Kuerten, and J.A.M. Kuipers. A critical comparison of smooth and sharp interface methods for phase transition. *International Journal of Multiphase Flow*, 120:103093, 2019.

27 B. Roman, E. Hamm, and F. Melo. Forbidden directions for the fracture of thin anisotropic sheets: An analogy with the Wulff plot. *Physical Review Letters*, 110, April 2013. doi:10.1103/PhysRevLett.110.144301.

28 A. Schlüter, A. Willenbücher, C. Kuhn, and R. Müller. Phase field approximation of dynamic brittle fracture. *Computational Mechanics*, 54:1141–1161, 2014.

29 C. Schreiber, C. Kuhn, and R. Müller. Phase field modeling of cyclic fatigue crack growth under mixed mode loading. *Computer Methods in Materials Science*, 19:50–56, 2019.

30 C. Schreiber, C. Kuhn, R. Müller, and T. Zohdi. A phase field modeling approach of cyclic fatigue crack growth. *International Journal of Fracture*, 2020.

31 M. Seiler, P. Hantschke, A. Brosius, and M. Kästner. A numerically efficient phase-field model for fatigue fracture – 1d analysis. *PAMM*, 18(1), 2018.

32 S. Teichtmeister, D. Kienle, F. Aldakheel, and M.A. Keip. Phase field modeling of fracture in anisotropic brittle solids. *International Journal of Non-Linear Mechanics*, pages 100–118, July 2017.

33 C. V. Verhoosel and R. de Borst. A phase-field model for cohesive fracture. *International Journal for Numerical Methods in Engineering*, 96(1):43–62, 2013.

34 A.A. Wheeler, B.T. Murray, and R.J. Schaefer. Computation of dendrites using a phase field model. *Physica D: Nonlinear Phenomena*, 66(1):243–262, 1993.

35 C. H. Wu. Maximum-energy-release-rate criterion applied to a tension-compression specimen with crack. *Journal of Elasticity*, 8:235–257, 1978.